Dalton Transactions

Accepted Manuscript

ROYAL SOCIETY OF CHEMISTRY

www.rsc.org/dalton

Pictogram of Graphical Abstract

Five Water-Soluble Zwitterionic Copper(II)-Carboxylate Polymers: Role of Dipyridyl Coligands in Enhancing the DNA-Binding, Cleaving and Anticancer Activities

Ming Chen, Xiao-Yan Tang, Shui-Ping Yang, Huan-Huan Li, Hai-Qing Zhao, Zhi-Hong Jiang, Wen-Hua Chen,* Jin-Xiang Chen*

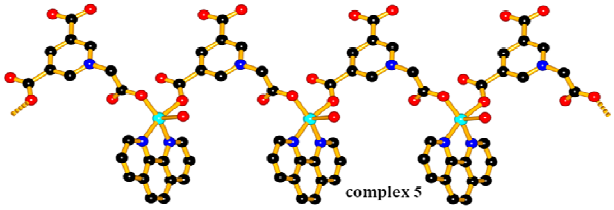

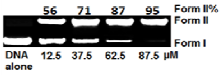

Cell	A549	MCF-7	HT-29	Hep-3B	HepG-2	A549/DDP
IC_{50} (μM)	0.35 ± 0.03	0.18 ± 0.07	1.16 ± 0.07	0.16 ± 0.05	0.24 ± 0.06	3.15 ± 0.24

Journal Name

ARTICLE

Five water-soluble zwitterionic copper(II)-carboxylate polymers: role of dipyridyl coligands in enhancing the DNA-binding, cleaving and anticancer activities

Ming Chen,[‡, a] Xiao-Yan Tang,[‡, b] Shui-Ping Yang,[a] Huan-Huan Li,[a] Hai-Qing Zhao,[a] Zhi-Hong Jiang,[c] Jin-Xiang Chen,*[a] Wen-Hua Chen*[a]

Cite this: Dalton Trans., xxxx, xx, xxxx

Received 00th January 20xx,

Accepted 00th January 20xx

DOI: 10.1039/x0xx00000x

www.rsc.org/

Five water-soluble zwitterionic copper-carboxylate polymers were prepared from the reaction of *N*-carboxymethyl-(3,5-dicarboxyl)pyridinium bromide (H_3CmdcpBr) with $Cu(NO_3)_2$ in the presence of NaOH, by modulating the temperature, solvent and ancillary dipyridyl ligands. These complexes include a 1D ladder-shaped polymer $\{[Cu_3(Cmdcp)_2(OH)_2(H_2O)_2]\cdot H_2O\}_n$ (**1**) formed in H_2O at room temperature, and a 2D network polymer $\{[Cu(Cmdcp)(H_2O)_2]\cdot 2H_2O\}_n$ (**2**) isolated in H_2O at 135 °C. At 100 °C in H_2O/DMF, the same reaction in the presence of an additional 2,2'-bipyridine (bipy) gave a 2D zwitterionic complex $\{[Cu(Cmdcp)(bipy)]\cdot 3H_2O\}_n$ (**3**), together with a 1D double-stranded polymer $\{[Cu(Cmdcp)(H_2O)_2]\cdot H_2O\}_n$ (**4**) as a minor product. Replacement of bipy with phenanthroline (phen) afforded a 1D zigzag chain polymer $\{[Cu(Cmdcp)(phen)(H_2O)]_2\cdot 9H_2O\}_5$ (**5**). All these complexes were characterized by IR, elemental analyses and single crystal X-ray crystallography. Agarose gel electrophoresis (GE) and ethidium bromide (EB) displacement experiments indicated that complex **5** exhibited the highest pBR322 DNA cleaving ability with the catalytic efficiency (k_{max}/K_M) of 14.80 $h^{-1}\cdot mM^{-1}$, and the highest binding affinity toward calf-thymus DNA. MTT assay indicated that complex **5** showed significant inhibitory activity toward the proliferation of several tumor cells. Its IC_{50} value was at micromolar level and lower than those of cisplatin and complexes **1**-**4**, especially toward resistant lung adenocarcinoma cell A549.

Introduction

Cisplatin, a metal-based anticancer drug, is one of chemotherapeutic agents currently used for treating various types of cancers like ovarian, testicular, head and neck carcinomas.[1] Though it is one of the most active anticancer drugs, its curative in some tumors is limited by its cytotoxicity, drug resistance and poor water solubility. Therefore, during the last few decades, considerable effort has been focused on the development of new anticancer drugs based on transitional metal complexes to achieve more-efficacious, less cytotoxic and target-specific DNA-binding anticancer drugs. [2] Among those potential candidates, biocompatible copper(II) complexes are identified to bind to and cleave DNA under physiological conditions. [3]

Copper is a biologically relevant element and is responsible for the activity of many enzymes. For this reason, a large number of copper(II) complexes have been synthesized and explored for their biological activities.[4] In particular, copper(II) complexes of polypyridyl ligands are attractive due to their high nucleolytic efficiency and anti-tumor activities.[5] It is known that polypyridyl ligands, such as 2,2'-bipyridine (bipy) and 1,10-phenanthroline (phen) (Scheme 1), are chelating ligands for transition metal ions.[6] Because of the planar, rigid and hydrophobic features of polypyridyl ligands, their copper complexes have been used as intercalating or groove binding agents for DNA, which may contribute to DNA cleaving and anti-tumor activities. [7]

In an earlier study, we have reported a water-soluble copper complex based on a zwitterionic carboxylate ligand, 4-carboxy-1-(4-carboxybenzyl)pyridinium bromide (H_2CcbpBr, Scheme 1). We have found that this copper complex showed moderate DNA-binding and cleaving activity due to its polymer structure. [8] In the work reported herein, we synthesized a zwitterionic carboxylate ligand with one more carboxylic group, that is, *N*-carboxymethyl-(3,5-dicarboxy)pyridinium bromide (H_3CmdcpBr, Scheme 1) and

[a] *Guangdong Provincial Key Laboratory of New Drug Screening, School of Pharmaceutical Sciences, Southern Medical University, Guangzhou 510515, P. R. China. Fax: +86-20-61648533; E-mail: jxchen@smu.edu.cn, whchen@smu.edu.cn*

[b] *Department of Chemistry and Materials Engineering, Jiangsu Key Laboratory of Advanced Functional Materials, Changshu Institute of Technology, Changshu 215500, Jiangsu, P. R. China*

[c] *Macau Institute for Applied Research in Medicine and Health, Macau University of Science and Technology, Taipa, Macau*

‡ *Ming Chen and Xiao-Yan Tang contributed equally to this work.*

†Electronic Supplementary Information (ESI) available: Selected bond distances (Å) and angles (°) for complexes **1**-**5**. The double layered structure linked by secondary bond of Cu···O in **1**. The effect of the addition of complexes **1**-**5** of varying concentrations on the emission intensity of the CT DNA-bound ethidium bromide (EB). Fluorescence decrease of EB induced by the competitive binding of complexes **1**-**5** to CT-DNA. Time courses of pBR322 DNA cleavage promoted by complexes **2**, **3** and **5**. Cleaving mechanism of complexes **2** and **3**. CCDC reference numbers 1058283-1058287 for complexes **1**-**5**. For ESI and crystallographic data in CIF format, see DOI:10.1039/c000000x/

introduced two DNA binding agents, bipy and phen into the copper polymers with the aim to improve the DNA-binding and cleaving activities. Herein, we report five water-soluble zwitterionic copper carboxylate polymers $\{[Cu_3(Cmdcp)_2(OH)_2(H_2O)_2]\cdot H_2O\}_n$ (**1**), $\{[Cu(Cmdcp)(H_2O)_2]\cdot 2H_2O\}_n$ (**2**), $\{[Cu(Cmdcp)(bipy)]\cdot 3H_2O\}_n$ (**3**), $\{[Cu(Cmdcp)(H_2O)_2]\cdot H_2O\}_n$ (**4**) and $\{[Cu(Cmdcp)(phen)(H_2O)]_2\cdot 9H_2O\}_n$ (**5**) and their DNA binding, cleaving and anticancer activities.

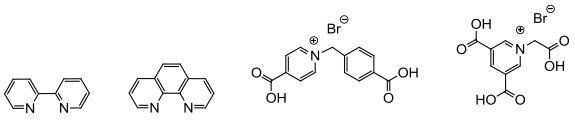

Scheme 1. Structures of bipy, phen, H_2CcbpBr and H_3CmdcpBr.

Experimental

General procedures. IR spectra were recorded on a Nicolet MagNa-IR 550. Elemental analyses for C, H, and N were performed on an EA1112 CHNS elemental analyzer. Agarose gel electrophoresis (GE) was conducted on a DYY-8C electrophoresis apparatus and DYCP-31DN electrophoresis chamber, and detected on an Alpha Hp 3400 fluorescence and visible light digital image analyzer. UV-Vis and fluorescence spectra were measured on a TU-1901 spectrophotometer and a HITACHI F-2500 spectrofluorimeter, respectively.

Calf-thymus (CT) DNA and plasmid pBR322 DNA were purchased from Sigma-Aldrich and Takara Chemical Co., respectively. Their solutions were prepared in 5 mM Tris-HCl buffer (5 mM NaCl, pH 7.0). The concentration of CT DNA was determined spectrophotometrically using the molar extinction coefficient of 13,200 $M^{-1}\cdot cm^{-1}$ per base pair (bp) at 260 nm.[9] All the other chemicals and reagents were obtained from commercial sources and used without further purification. H_3CmdcpBr was synthesized according to the method we reported.[10] Buffer solutions were prepared in triply distilled deionized water.

Synthesis of complexes 1-5

Preparation of solution 1: H_3CmdcpBr (61 mg, 0.2 mmol) was suspended in MeOH (5 mL), and the pH was adjusted to 7.0 with 0.1 M NaOH solution to give a clear solution. Then, a solution of $Cu(NO_3)_2\cdot 3H_2O$ (48 mg, 0.2 mmol) in MeOH (5 mL) was added, and the resulting mixture was stirred for 30 min. After stirring for 30 min, the formed green precipitates were collected by filtration, washed with MeOH (5 mL), and then dissolved in H_2O (30 mL) at room temperature. The resulting mixture was filtered to afford a clear green solution.

$\{[Cu_3(Cmdcp)_2(OH)_2(H_2O)_2]\cdot H_2O\}_n$ (1). The above prepared clear green solution 1 was allowed to stand at room temperature for two weeks to give blue crystals. The resulting crystals were collected, washed with MeOH and dried *in vacuo* to give complex **1** (43 mg, 89%). Anal. Calcd. for $C_{18}H_{18}Cu_3N_2O_{17}$: C 29.82, H 2.50, N 3.86. Found: C 29.79, H 2.66, N 3.75 and IR (KBr disc, cm^{-1}) *v* 3437 (s), 2998 (s), 1655 (s), 1633 (s), 1601 (s), 1459 (w), 1397 (s), 1382 (s), 1353 (s), 1307 (m), 1241 (w), 1175 (w), 1094 (s), 935 (w), 770 (s), 729 (s), 650 (m), 479 (w).

$\{[Cu(Cmdcp)(H_2O)_2]\cdot 2H_2O\}_n$ (2). The above solution 1 was transferred to a Teflon reactor, sealed in an autoclave and then placed in a programmable oven. The temperature of the oven was increased steadily from 25 ºC to 135 ºC within 4 h, kept at 135 ºC for 72 h and then cooled to room temperature within 48 h to give green crystals. The resulting crystals were collected, washed with MeOH and dried *in vacuo* to give complex **2** (64 mg, 90%). Anal. Calcd. for $C_9H_{13}CuNO_{10}$-H_2O: C 31.72, H 3.25, N 4.11. Found: C 31.93, H 3.10, N 3.97 and IR (KBr disc, cm^{-1}) *v* 3437 (s), 3083 (m), 2998 (s), 1655 (s), 1633 (s), 1601 (s), 1459 (m), 1397 (s), 1382 (s), 1353 (s), 1307 (m), 1241 (m), 1175 (m), 1094 (s), 770 (s), 729 (s), 650 (m), 479 (m).

$\{[Cu(Cmdcp)(bipy)]\cdot 3H_2O\}_n$ (3) and **$\{[Cu(Cmdcp)(H_2O)_2]\cdot H_2O\}_n$ (4)**. The above solution 1 was treated with bipy (31 mg, 0.2 mmol) in DMF (5 mL) at 100 °C to give a green solution. The solution was stirred for 0.5 h and filtered. The filtrate was allowed to stand at ambient temperature for several days to give dark blue crystals **3** coupled with light green crystals **4**, which were separated mechanically under the microscope. Complex **3**: 46 mg (46%). Anal. Calcd. for $C_{19}H_{19}CuN_3O_9$: C 45.92, H 3.85, N 8.46. Found: C 46.09, H 3.96, N 8.37 and IR (KBr disc, cm^{-1}) *v* 3381 (s), 3020 (s), 1657 (s), 1602 (s), 1570 (m), 1499 (m), 1474 (m), 1447 (s), 1426 (m), 1402 (s), 1385 (s), 1359 (s), 1313 (s), 1301 (s), 1235 (m), 1177 (m), 1158 (w), 1064 (w), 1032 (m), 918 (m), 780 (s), 724 (s), 658 (m), 617 (m). Complex **4**: 21 mg (31%). Anal. Calcd. for $C_9H_{11}CuNO_9$: C 31.72, H 3.25, N 4.11. Found: C 31.44, H 3.18, N 3.93 and IR (KBr disc, cm^{-1}) *v* 3566 (s), 3470 (s), 3372 (s), 3077 (s), 1657 (s), 1603 (s), 1488 (w), 1451 (m), 1384 (s), 1371 (s), 1324 (s), 1299 (s), 1242 (s), 1181 (m), 940 (w), 916 (w), 832 (w), 769 (s), 732 (s), 645 (s), 462 (m).

$\{[Cu(Cmdcp)(phen)(H_2O)]_2\cdot 9H_2O\}_n$ (5). The above solution 1 was treated with phen (36.0 mg, 0.2 mmol) in DMF (5 mL) to give a green solution accompanied by some blue precipitates. The mixture was heated at 100 ºC for 0.5 h (to dissolve the blue precipitates) and then filtered. The filtrate was allowed to stand at ambient temperature for several days to give blue crystals. The resulting crystals were collected, washed with MeOH and dried *in vacuo* to give complex **5** (100 mg, 92%). Anal. Calcd. for $C_{42}H_{44}Cu_2N_6O_{21}$: C 46.03, H 4.05, N 7.67. Found: C 46.10, H 4.02, N 7.43. IR (KBr disc, cm^{-1}) *v* 3405 (s), 3067 (s), 1649 (s), 1617 (s), 1599 (s), 1518 (m), 1425 (s), 1407 (m), 1375 (s), 1363 (s), 1291 (w), 1234 (m), 1172 (w), 1141 (w), 1107 (m), 848 (m), 774 (s), 736 (s), 722 (m), 639 (m).

X-ray crystal structure determinations. All the measurements were made on a Bruker AXS APEX II diffractometer by using graphite-monochromated Mo Kα (λ = 0.71073 Å). The data were subjected to empirical absorption correction using SADABS.[11] All the crystal structures were solved by direct methods and refined on F^2 by full-matrix least-squares techniques with SHELXTL–97 program.[12]

In complex **1**, the hydrogen atoms on H_2O molecules and OH groups were located from the difference Fourier map with their O–H distances restrained to be equal and thermal parameters constrained to $U_{iso}(H) = 1.2U_{eq}(O)$. In complex **2**, the occupancy factor for O3W and O4W was fixed at 0.5 to obtain reasonable thermal factors. The hydrogen atoms on the two coordinated H_2O molecules were located from the difference Fourier map with their O–H distances restrained

to 0.85 Å and thermal parameters constrained to U_{iso}(H) = 1.2U_{eq}(O). The location of the hydrogen atoms on dissociated water was suggested by Calc-OH program in WinGX suite and refined as rigid group with O–H = 0.85 Å and thermal parameters U_{iso}(H) = 1.2U_{eq}(O).[13] In complexes **3** and **4**, all the hydrogen atoms on the H_2O molecules were located from the difference Fourier map with their O–H distances restrained to 0.85 Å and thermal parameters constrained to U_{iso}(H) = 1.2U_{eq}(O). In complex **5**, O5W lies on a special position of higher symmetry than that the molecule itself can possess. It is treated as spatial disorder but applying PART –1 and PART 0 in the .ins file with the site occupation factors changed to 0.50 for the atoms. The hydrogen atoms on the two H_2O molecules were located from the difference Fourier map. For O2W and O3W, their O–H distances restrained to 0.85 Å and thermal parameters constrained to U_{iso}(H) = 1.2U_{eq}(O). For O1W, O4W and O5W, the water molecules are refined as a rigid model. The key crystallographic information for complexes **1**-**5** was summarized in Table 1. Selected bond lengths and angles are listed in Table S1 in the electronic supplementary information (ESI).

Table 1 Crystallographic data for complexes **1**-**5**

Complex	**1**	**2**	**3**	**4**	**5**
Molecular formula	$C_{18}H_{18}Cu_3N_2O_{17}$	$C_9H_{13}CuNO_{10}$	$C_{19}H_{19}CuN_3O_9$	$C_9H_{11}CuNO_9$	$C_{42}H_{44}Cu_2N_6O_{21}$
Formula weight	724.96	358.74	496.91	340.73	1086.21
Crystal system	triclinic	monoclinic	monoclinic	triclinic	triclinic
Space group	*P-1*	$P2_1/c$	$P2_1/n$	*P-1*	*P-1*
a (Å)	8.5827(3)	9.2384(18)	9.1905(5)	7.1654(9)	8.6748(17)
b (Å)	10.6301(4)	7.4454(15)	7.7875(4)	7.6594(9)	11.213(2)
c (Å)	13.4395(5)	23.041(6)	27.5073(15)	11.4555(14)	12.653(3)
α (°)	95.3540(10)	90.00	90.00	77.713(2)	112.47(3)
β (°)	95.6380(10)	113.23(3)	94.0020(8)	75.932(2)	93.34(3)
γ (°)	112.3110(10)	90.00	90.00	74.525(2)	99.01(3)
V (Å^3)	1117.45(7)	1456.4(6)	1963.92(18)	580.34(12)	1113.8(4)
Z	2	4	4	2	1
T/K	296(2)	153(2)	296(2)	296(2)	173(2)
D_{calc} (g cm^{-3})	2.155	1.636	1.681	1.950	1.619
λ (Mo-K*α*) (Å)	0.71073	0.71073	0.71073	0.71073	0.71073
μ(cm^{-1})	2.926	1.548	1.173	1.931	1.048
Total reflections	21401	14424	14396	4395	7056
Unique reflections	6027	3336	4016	2370	3782
No. observations	5167	2704	3651	2257	3430
No. parameters	387	211	289	199	337
R^a	0.0303	0.0549	0.0337	0.0326	0.0707
wR^b	0.0797	0.1593	0.0980	0.0863	0.1791
GOF^c	1.051	1.113	0.744	1.081	1.148
$\Delta\rho_{max}$(e Å^{-3})	0.666	1.220	0.539	1.372	3.027
$\Delta\rho_{min}$ (e Å^{-3})	-0.730	-0.532	-0.569	-0.988	-0.634

$^aR = \Sigma||F_c|-|F_c|/\Sigma|F_o||$. $^bwR = \{\Sigma w(F_o^2-F_c^2)^2/\Sigma w(F_o^2)^2\}^{1/2}$. ^{c} GOF = $\{\Sigma w((F_o^2-F_c^2)^2)/(n-p)\}^{1/2}$, where n = number of reflections and p = total numbers of parameters refined.

DNA cleavage experiments. The cleavage experiments were conducted at 37 °C, in 5 mM Tris-HCl buffer (5 mM NaCl, pH 7.0), by using the methods similar to those described previously.[14] Specifically, a mixture of pBR322 DNA (0.5 g/L, 0.7 μL) and each of complexes **1**-**5** of varying concentrations was diluted with 5 mM Tris-HCl buffer (5 mM NaCl, pH 7.0) to 16 μL and incubated at 37 °C for 5 h. The reaction was quenched by adding 10 mM Tris-HCl loading buffer (pH 7.6) containing 0.03% bromophenol blue, 60% glycerol, 60 mM EDTA and 0.03% xylene cyanol FF. The reaction mixture was then loaded on 1% agarose gel containing ethidium bromide (EB) (1.0 mg/L), and analyzed with gel electrophoresis in Tris-acetate (40 mM)-EDTA (1.0 mM) (TAE) buffer (pH 8.0) at 90 V. Bands were visualized by UV light and photographed for analysis. The extent of the cleavage of the supercoiled DNA was determined by measuring the intensities of the bands using the Alpha Innotech gel documentation system (Alpha Hp3400).

The kinetics for the DNA cleavage was investigated at different intervals of time, by varying the concentrations of complexes **2**, **3** and **5**. The percentage of the supercoiled DNA was plotted against time for each concentration of complexes **2**, **3** and **5**. The data were fitted with a single-exponential curve (*pseudo* first-order kinetics) to give the k_{obs} values, which were then plotted against the concentrations of each complex (Eq. (1)) to afford the corresponding maximal first-order rate constant k_{max} and the Michaelis constant K_M.

$$k_{obs} = k_{max}[\text{metal complex}]/(K_M + [\text{metal complex}]) \quad (1)$$

For mechanistic investigations, experiments were carried out in a similar fashion, except in the presence of DMSO (1.0 M), MeOH (1.0 M), NaN_3 (0.1 M), KI (0.1 M) and EDTA (0.1 M), followed by addition of each of complexes **2**, **3** and **5**.

DNA binding experiments. *EB displacement experiments* of H_3CmdcpBr, $Cu(NO_3)_2$ and complexes **1-5** were performed by keeping the concentrations of CT DNA and EB constant, while gradually increasing the concentration of each metal complex. Specifically, to a solution of CT DNA (2.40 μM) and EB (3.03 μM) in 5 mM Tris-HCl (5 mM NaCl, pH 7.0) were added aliquots of a solution of each complex containing CT DNA (2.40 μM) and EB (3.03 μM) in the same buffer. The corresponding fluorescence spectra were measured (λ_{ex} = 510 nm) until saturation was observed. The apparent binding constant (K_a) was obtained by analyzing the relative fluorescence intensity (I/I_0, λ_{em} = 590 nm) as a function of the concentrations of each complex. [15]

MTT assay. The cytotoxicities of complexes **1**-**5** and cisplatin as a positive control toward several human cancer cell lines were investigated, by using an MTT assay.[16] Briefly, (3-8)×10^3 cells/well were seeded in 96-well microplates in growth medium (100 μL). After 24 h, the medium was removed and replaced with fresh media containing a complex of appropriate concentration. After 24 h, each well was treated with 10 μL of a 5 mg/mL MTT saline solution. After 4 h of incubation, 100 μL DMSO was added to each well. Cell growth inhibition was detected by measuring the absorbance of each well at 570 nm using the GENios Pro microplate reader (TECAN). Each experiment was carried out three times, and the mean values were taken.

Results and discussion

The reaction condition for each complex is summarized in Scheme 2. Five water-soluble copper polymers were prepared from the reaction of H_3CmdcpBr with $Cu(NO_3)_2$ in the presence of NaOH, by modulating the temperature, solvent and ancillary bipyridyl ligands. This verified literature report that different synthetic conditions would lead to the formation of different coordination complexes.[17] In the present case, complex **1** may be a kinetic product, whereas complexes **2** and **4** are thermodynamic products.[18] Complexes **1**-**5** are air and moisture stable. Upon ultrasonication, complexes **1**-**5** show good water solubility with maximum concentrations being up to 1.0 mM for **1**, **2**, **4** and **5**, and 2 mM for **3**, respectively. This water solubility is much greater than that of cisplatin (8×10^{-3} mM) and high enough for most bioactivity study. [19]

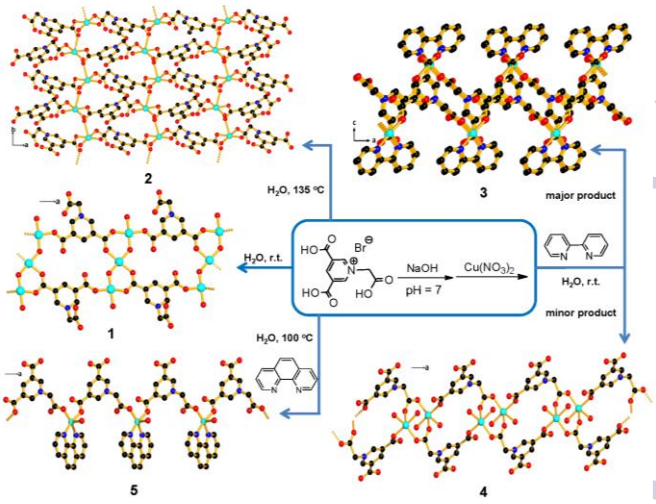

Scheme 2. Pathway to the synthesis of complexes **1**-**5**. Color codes: Cu (turquiose), O (red), N (blue), C (black).

Crystal structure of $\{[Cu_3(Cmdcp)_2(OH)_2(H_2O)_2]\cdot H_2O\}_n$ (1). Complex **1** crystallizes in triclinic space group *P*ī and the asymmetric unit consists of one $[Cu_3(Cmdcp)_2(OH)_2(H_2O)_2]$ molecule and one dissociated H_2O molecule. In complex **1**, the adjacent two copper (II) atoms in the linear Cu_3 subunit are linked by one *μ*-OH group and each terminal copper atom further coordinate to one H_2O molecule, thereby forming a $[Cu_3(OH)_2(H_2O)_2]$ unit. A couple of Cmdcp ligands linked two of these subunits through one monodentate carboxylate coordinating to one terminal Cu(II) ion in one $[Cu_3(OH)_2(H_2O)_2]$ subunit and one *μ*-chelating carboxylate coordinating to the neighboring subunit, alternatively, thereby forming a one-dimensional ladder-like structure as shown in Scheme 2. Secondary bond of Cu···O (Cu···O^i = 2.639 (2) Å, symmetric code: i = 2 - *x*, 1 - *y*, 1- *z*) between the adjacent ladder-shaped layers link the two ladders into a double-ladder structure (Fig. S1). Three crystallographically independent copper atoms Cu(1), Cu(2) and Cu(3) within the ladder are all square planar coordination. The central Cu(2) atom, being located at a crystallographic inversion center, is coordinated by four oxygen atoms, two of them from *μ*-carboxylato bridges of Cmdcp ligands and the other two from *μ*-hydroxo bridges. The tetra-coordination of two terminal copper atoms Cu(1) and Cu(3) complete by one *μ*-carboxylate bridge atom, one monodentate carboxylate group, one *μ*-hydroxo bridge and one H_2O molecular. In complex **1**, the average Cu-O (water) bond length of 1.9466(10) Å is comparable to that of Cu-O (carboxylate) (1.9107 (17) Å), but shorter than that of the Cu-O (water) bond in complex $[Cu(II)L(H_2O)]I_2$ (2.430(0) Å, H_4L = [5,11,17,23-tetrakis (trimethylammonium)-25,26,27,28-tetrahydroxycalix[4]arene]),[20] indicating that the water molecules interact tightly with the Cu(II) centers.

Crystal structure of $\{[Cu(Cmdcp)(H_2O)_2]\cdot 2H_2O\}_n$ (2). Complex **2** crystallizes in monoclinic space group $P2_1/c$ and the asymmetric unit consists of one $\{[Cu(Cmdcp)(H_2O)_2]$ molecule and two solvated H_2O molecules. Single-crystal X-ray analysis of complex **2** reveals the formation of a 2D network polymer along *ab* plane. As shown in Scheme 2, each Cu^{2+} center exhibits a square pyramidal geometry surrounded by five O atoms, of which two are

from two H_2O molecules and the other three from two monodentate carboxylates and one bridging carboxylate of three different Cmdcp ligands. Each Cmdcp ligand connects three Cu^{2+} ions in which the first carboxylate acts as a monodentate coordination mode and the second one a *cis-trans* bidentate coordination mode, while the third carboxylate is free and deprotonated to balance the positive charge of the pyridinum cation and Cu(II) center. In complex **2**, the Cu(1)-O(2) bond length of 2.425(3) Å is longer than those of other Cu-O bond lengths from 1.937(3) to 1.970(3) Å, and also longer that of one in complex [CuL(bbm)]·0.5H_2O (1.983(2) Å; H_2L = 4,4'-{[1,2-phenylenebis(methylene)]bis(oxy)}dibenzoic acid, bbm =1,4-di(1H-imidazol-1-yl)benzene),[21] implying the weak interaction between Cu1 and O2 from one carboxylate group.

Crystal structure of {[Cu(Cmdcp)$_2$(bipy)]·2H_2O}$_n$ (3). Complex **3** crystallizes in monoclinic space group $P2_1/n$ and the asymmetric unit consists of one [Cu(Cmdcp)$_2$(bipy)] molecule and two solvated H_2O molecules. In complex **3**, each Cmdcp ligand shows a tri-monodentate coordination mode to connect three adjacent cooper(II) ions, thereby forming a two dimensional network structure along *ab* plane (Fig. S2). This two dimensional structure is constructed by boat-type macrocylic rings which is formed by [Cu_3(Cmdcp)$_3$] units. Each copper(II) is coordinated to three monodentate carboxylates from three Cmdcp ligands and further to two nitrogen atoms from bipy (Scheme 2), thereby forming tetragonal pyramidal coordination geometry. In complex **3**, the mean Cu-O and Cu-N bond lengths (1.945(3) Å *vs* 2.008(12) Å) are comparable to the corresponding ones found in [CuL(bbm)]·0.5H_2O (1.983(5) Å vs 1.977(5) Å).[21]

Crystal structure of {[Cu(Cmdcp)(H$_2$O)$_2$]·H$_2$O}$_n$ (4). Complex **4** crystallizes in triclinic space group $P\bar{1}$ and the asymmetric unit consists of one [Cu(Cmdcp)(H_2O)$_2$] molecule and one dissociated H_2O molecule. As depicted in Scheme 2, the Cu atoms forms a dimeric cluster unit and further extended along the *a* axis through the Cmdcp ligand pairs to form a one-dimensional chain. In the Cmdcp ligand, the first carboxylate bridged the two Cu atoms in the clusters unit while the other two are monodentate and uncoordinated to balance the positive charge of the pyridinum cation and Cu(II) center. Each copper(II) in turn is coordinated to five oxygen atoms from three Cmdcp ligands and two water, forming a trigonal bipyramidal coordination geometry. In complex **4**, the Cu(1)-O(5) bond length of 2.293(2) Å is longer than other Cu-O bond lengths from 1.932(19) to 1.989(13) Å, implying the weak interaction between Cu1 and O5 from one carboxylate group.

Crystal structure of {[Cu(Cmdcp)(phen)(H$_2$O)]·4H$_2$O}$_n$ (5). Complex **5** crystallizes in triclinic space group $P\bar{1}$ and the asymmetric unit consists of one [Cu(Cmdcp)(phen)(H_2O)] molecule and four dissociated H_2O molecules. As depicted in Scheme 2, each copper(II) ion coordinates to two nitrogen atoms from one phen ligand and one oxygen atom from one H_2O molecule to form a [Cu(phen)(H_2O)] unit. This unit was connected by di-monodentate Cmdcp ligands to form one dimensional chain structure along *a* axis. The third carboxylate group shows a free group to balance the positive charge of the pyridinum cation and Cu(II) center. In complex **5**, the five-coordinated Cu^{2+} center exhibits a square pyramidal geometry. In complex **5**, the Cu(1)-O (1W) bond length of 2.271(4) Å is longer than the mean Cu-O (carboxylate) bond length (1.950 (4) Å), implying that the H_2O weakly coordinates to the Cu(II) centre. The mean Cu-N bond length of 2.023(12) Å is comparable to the one found in complex **3** (2.008(12) Å).

DNA cleavage study. It is reported that metal complexes are capable of catalyzing the cleavage of DNA.[22] Therefore, we firstly examined whether complexes **1**-**5** exhibited DNA-cleaving activities by using agarose GE assay. Fig. 1 shows the GE patterns for the cleavage of supercoiled pBR322 DNA by complexes **1**-**5**, H_3CmdcpBr and Cu(NO_3)$_2$ at pH 7.0 and 37 °C. It can be seen that complexes **3** and **5** with ancillary bipy and phen ligands could efficiently relax the supercoiled form (Form I) of DNA into an open circular form (Form II) (Lanes 4 and 6) with the percentage of Form II being 85% and 96%, respectively. Complexes **1**, **2** and **4** without ancillary ligands showed relatively low cleaving activities. It should be noted that under the same condition, H_3CmdcpBr and Cu(NO_3)$_2$ showed no detectable cleaving activity.

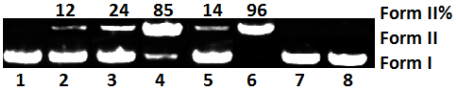

Fig. 1. Agarose GE patterns for the cleavage of pBR322 DNA by complexes **1**-**5**, H_3CmdcpBr and Cu(NO_3)$_2$ (87.5 μM) at pH 7.0 at 37 °C. Lane 1: DNA alone; Lanes 2-8: DNA with complexes **1**, **2**, **3**, **4**, **5**, H_3CmdcpBr and Cu(NO_3)$_2$, respectively.

Secondly, we carried out the DNA cleavage by complexes **1**-**5** of varying concentrations. It can be seen from Fig. 2 that complexes **3** and **5** are capable of converting supercoiled pBR322 DNA into open circular form in a concentration-dependent fashion. Complex **2** exhibited certain concentration-dependent, but obviously much lower activity. However, complexes **1** and **4** showed no obvious concentration-dependence. Therefore, we further investigated the DNA-cleaving activities of complexes **2**, **3** and **5**.

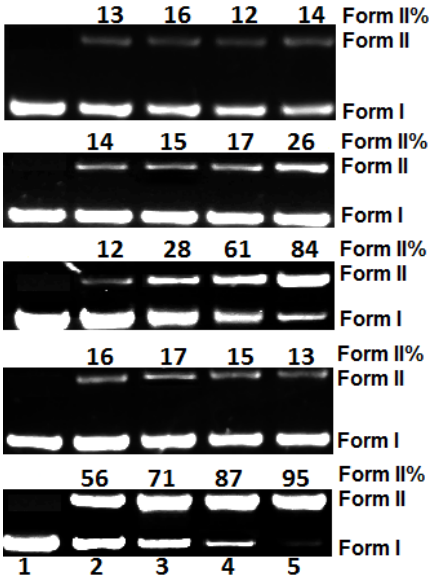

Fig. 2. Agarose GE patterns for the cleavage of pBR322 DNA by complexes **1**-**5** (from top to bottom) at pH 7.0 and 37 °C for 5 h.

Lane 1: DNA alone; Lanes 2-5: DNA with complexes at the concentrations of 12.5, 37.5, 62.5, 87.5 μM, respectively.

To gain further insight into the cleaving activities of complexes **2**, **3** and **5**, we studied the kinetics of pBR322 DNA degradation.[23] As a result, the maximal first-order rate constants (k_{max}'s) and the Michaelis constants (K_M's) obtained from the saturation kinetic profiles of the supercoiled DNA cleavage, were 0.28 ± 0.01 h^{-1} and (371.8 ± 50) μM for **2**, 0.52 ± 0.07 h^{-1} and 103.67 ± 24.22 μM for **3**, 0.74 ± 0.09 h^{-1} and 50.01 ± 13.11 μM for **5**, respectively (Fig. 3). Thus, the catalytic efficiency (k_{max}/K_M) is 1.75 $\mu M^{-1}\cdot h^{-1}$ for complex **2**, 5.05 $\mu M^{-1}\cdot h^{-1}$ for complex **3** and 14.8 $\mu M^{-1}\cdot h^{-1}$ for complex **5**, respectively, indicating that complexes **3** and **5** are much more active than complex **2**. In particular, complexes **3** and **5** can catalyze the cleavage at a rate acceleration of *ca.* 1.4×10^7 and 2.0×10^7 folds over uncatalyzed supercoiled DNA cleavage (k = 3.6×10^{-8} h^{-1} for cleavage of a phosphodiestier bond in double-stranded DNA under physiological condition), respectively. [24] It is noteworthy that complexes **3** and **5** exhibit higher catalytic efficiency than our reported carboxylate Cu(II) complexes $[Cu(CBB)_2](NO_3)_2\cdot2H_2O$ (0.91 $\mu M^{-1}\cdot h^{-1}$, CBB = 9-*O*-(4-carboxybenzyl)berberine).[25]

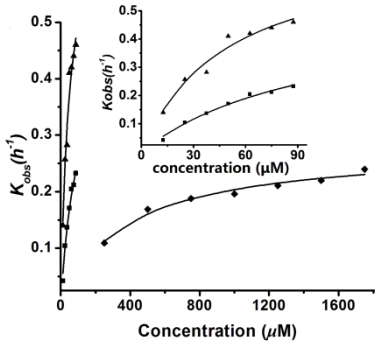

Fig. 3. Plots of k_{obs} versus the concentrations of complexes **2** (◆), **3** (■) and **5** (▲). Inset: Plots of k_{obs} versus the concentrations of complexes **2**(◆) and **3** (■) with an expanded *x*-axis.

It is widely recognized that DNA binding is a critical step for DNA cleavage in most cases. Thus, the above-mentioned outstanding acceleration shown by complexes **3** and **5** is a likely consequence of the presence of bipy and phen as DNA binding units. To test this hypothesis, we measured the binding affinities toward CT DNA of H_3CmdcpBr and complexes **1-5** by means of EB displacement experiment (Table 2). From the binding constant of H_3CmdcpBr ($(8.0 \pm 1.5)\times10^3$ M^{-1}) and $Cu(NO_3)_2$ ($(1.2 \pm 0.1)\times10^5$ M^{-1}) (Table 2 and Fig. 4a), we speculate that Cu^{2+} may play a major role in the DNA binding affinities of complexes **1-5**. In addition, complexes **3** and **5** showed higher binding affinities than complexes **1**, **2** and **4**, parallel to their DNA cleaving activities. Thus, the presence of bipy and phen as DNA-binding units may contribute a lot to the enhanced DNA-binding and cleaving affinity. [7]

Cleaving mechanism of action. It is known that DNA can be cleaved through an oxidative or hydrolytic pathway. In general, oxidative cleavage of plasmid DNA may lead to the formation of reactive singlet oxygen ($^1O_2$), hydrogen peroxide (H_2O_2) and/or hydroxyl radical (HO·) species. These species may cause damage to the sugar and/or base.[26] Meanwhile, in a hydrolytic cleavage pathway, the hydrolysis of the phosphodiester backbone of DNA may be enhanced.[27] To verify whether reactive oxygen species are, at least in part, responsible for the cleavage of pBR322 DNA, we conducted the cleavage reactions of complex **5** in the presence of hydroxyl radical scavengers DMSO and MeOH, singlet oxygen scavenger NaN_3, hydrogen peroxide scavenger KI and metal ion-chelating agent EDTA. As shown in Fig. 4b, EDTA efficiently inhibited DNA cleavage (Lane 7), suggesting that complexation of $Cmdcp^{2-}$ with copper ions is crucial to the cleavage. When DMSO (Lane 3), MeOH (Lane 4) or NaN_3 (Lane 6) was added, no significant influence on the DNA cleavage was observed, ruling out the possibility that hydroxyl radical and/or singlet oxygen were involved in the DNA cleavage. When KI was added, the DNA cleavage was significantly inhibited (Lane 5), suggesting that H_2O_2 might be the reactive species in the cleavage process. Taken together, these results strongly suggest that DNA cleavage by complex **5** proceeded, probably *via* an oxidative mechanism involving H_2O_2 species. Complexes **2** and **3** showed similar effects under the measuring conditions (supporting information, Fig. S34 and S35).

Table 2. Kinetic parameters and apparent binding constants K_a of complexes **1-5**

Complex	k_{max} (h^{-1})	K_M (mM)	k_{max}/K_M ($h^{-1}\cdot mM^{-1}$)	K_a (M^{-1})
H_3CmdcpBr	\	\	\	$(8.0 \pm 1.5) \times 10^3$
$Cu(NO_3)_2$	\	\	\	$(1.2 \pm 0.1) \times 10^5$
1	\	\	\	$(3.9 \pm 0.6) \times 10^5$
2	0.28 ± 0.01	0.382 ± 0.051	1.75	$(7.2 \pm 1.2) \times 10^5$
3	0.52 ± 0.08	0.104±0.024	5.05	$(1.2 \pm 0.2) \times 10^6$
4	\	\	\	$(5.5 \pm 0.7) \times 10^5$
5	0.74 ± 0.09	0.050 ± 0.013	14.8	$(2.8 \pm 0.7) \times 10^6$

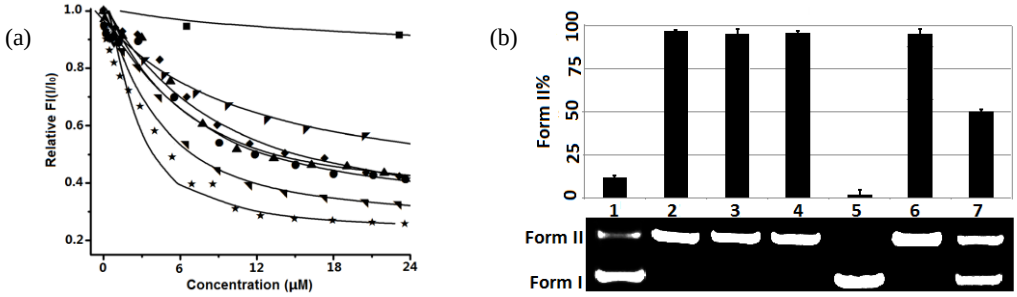

Fig. 4. (a) Fluorescence decrease of EB induced by the competitive binding of H_3CmdcpBr (■), $Cu(NO_3)_2$ (◤), complex **1** (●), complex **2** (▲), complex **3** (◥), complex **4** (◆) and complex **5** (★) to CT-DNA in 5mM Tris-HCl/NaCl buffer (pH 7.0) at room temperature (λ_{ex} = 510 nm, λ_{em} = 588 nm). (b) Agarose GE patterns for the cleavage of pBR322 DNA by complex **5** (87.5 μM) at pH 7.0 and 37 °C for 5 h, in the presence of DMSO (1 M, Lane 3), MeOH (1 M, Lane 4), KI (0.1 M, Lane 5), NaN_3 (0.1 M, Lane 6) and EDTA (0.1 M, Lane 7). Lane 1, DNA alone and Lane 2: DNA + complex **5**.

3.5. MTT assay

To exploit the potential application of complexes **1**-**5** in the development of antitumor agents, we evaluated their biological activities against the proliferation of breast (MCF-7), colon (HT-29), liver (Hep-3B), liver (HepG-2) and lung (A549) cancer cell lines, by using MTT assay.[28] The cytotoxicity parameters, in terms of IC_{50} obtained after 24 h exposure, are listed in Table 3. For comparison, the cytotoxicity of cisplatin was assessed under the same experimental conditions. It is clear that complexes **3** and **5** showed potent cytotoxic activity with the IC_{50} values markedly lower than those of complexes **1**, **2** and **4**. In particular, complex **5** showed significant antitumor activity with the IC_{50} value in the micromolar range, even lower than that of cisplatin. This clear-cut enhanced cell-killing effect may be ascribed to the coordination of bipy or phen. It is noteworthy that **5** distinguished itself as the most promising complex promoting a growth inhibitory effect that exceeded that of cisplatin by a factor ranging from 17 (Hep-3B liver cancer cells) to 163 (MCF-7 breast cancer cells). In addition, the antiproliferative activities of complexes **1**-**5** were also investigated in cisplatin-resistant cell lines (A549/DDP). Of all the complexes, once again **5** was found to be the most potent complex, with the IC_{50} value in low micromolar range, markedly lower than that recorded with cisplatin. Interestingly, the IC_{50} values of complex **5** toward A549 and MCF-7 (0.35 ± 0.03 μM *vs* 0.18 ± 0.07 μM) are comparable to those of some reported copper complexes containing phen ligands, such as [CuCl(phen)(PCN)] (0.68 ± 0.20 μM *vs* 0.31 ± 0.21 μM) and [CuBr(phen)(PCN)] (0.79 ± 1.23 μM *vs* 1.23 ± 0.74 μM; PCN = tris-(2-cyanoethyl) phosphine). [29]

Table 3. Cytotoxicities (IC_{50}, μM) of complexes **1**-**5** and cisplatin [a]

	IC_{50} ± SD					
Complex	A549	MCF-7	HT-29	Hep-3B	HepG-2	A549/DDP
1	>90	>90	>90	90.02 ± 12.25	>90	>90
2	>90	>90	>90	>90	>90	>90
3	>90	>90	4.02 ± 0.07	4.74 ± 1.03	8.91 ± 1.18	>90
4	>90	>90	>90	>90	>90	>90
5	0.35 ± 0.03	0.18 ± 0.07	1.16 ± 0.07	0.16 ± 0.05	0.24 ± 0.06	3.15 ± 0.24
Cisplatin	18.82 ± 0.72	29.48 ± 0.43	22.39 ± 0.54	2.71 ± 0.07	29.85 ± 0.40	>90

[a]IC_{50} = concentration of the drug required to inhibit growth of 50% of the cancer cells (μM). The data are mean ± SD of three replicates each.

Conclusions

In summary, five water-soluble zwitterionic copper carboxylate polymers **1**-**5** have been synthesized and characterized. Agarose GE studies indicated that complexes **3** and **5** were capable of efficiently converting supercoiled pBR322 DNA into OC forms, most probably *via* an oxidative cleavage mechanism and exhibited catalytic efficiencies (k_{max}/K_M) of 5.02 $h^{-1}\cdot mM^{-1}$ and 14.80 $h^{-1}\cdot mM^{-1}$, respectively. The results support the fact that the bipy or phen ring plays a major role in governing the nature of binding and cleaving DNA. MTT assay indicated that complex **5** showed significant *in vitro* antitumor activity, especially toward resistant cancer cells, with the IC_{50} value in the micromolar range, lower than those of cisplatin and complexes **1**-**4**. Thus, copper(II) complexes with phen as a co-ligand may have the potential

application in the development of anticancer drugs.

Acknowledgment

This work was financially supported by the National Natural Science Foundation of China (No. 21102070) and the Program for Pearl River New Stars of Science and Technology in Guangzhou (No. 2011J2200071) and South Medical University.

Notes and references

1 (a) Y. Jung, S. J. Lippard, *Chem. Rev*., 2007, **107**, 1387; (b) E. R. Jamieson, S. J. Lippard, *Chem. Rev*., 1999, **99**, 2467; (c) T. Boulikas, M. Vougiouka, *Oncol. Rep*., 2003, **10**, 1663.

2 (a) M. J. Rose, N. L. Fry, R. Marlow, L. Hinck, P. K. Mascharak, *J. Am. Chem. Soc*., 2008, **130**, 8834; (b) R. Ren, P. Yang, W. J. Zheng, Z. C. Hua, *Inorg. Chem*., 2000, **39**, 5454; (c) A. Hussain, D. Lahiri, M. S. A. Begum, S. Saha, R. Majumdar, R. R. Dighe, A. R. Chakravarty, *Inorg. Chem*., 2010, **49**, 4036; (d) V. G. Vaidyanathan, B. U. Nair, *Dalton Trans*., 2005, 2842; (e) V. Rajendiran, M. Murali, E. Suresh, S. Sinha, K. Somasundaram, M. Palaniandavar, *Dalton Trans*., 2008, 148; (f) E. Gao, M. C. Zhu, L. Liu, Y. Huang, L. Wang, C. Y. Shi, W. Z. Zhang, Y. G. Sun, *Inorg. Chem*., 2010, **49**, 3261; (g) M. Brindell, E. Kuli, S. K. C. Elmroth, K. Urban′ska, G. Stochel, *J. Med. Chem*., 2005, **48**, 7298.

3 (a) C. G. Hartinger, A. A. Nazarov, S. M. Ashraf, P. J. Dyson, B. K. Keppler, *Curr. Med. Chem*., 2008, **15**, 2574; (b) A. Grau-Campistany, A. Massaguer, D. Carrion-Salip, F. Barragán, G. Artigas, P. López-Senín, V. Moreno, V. Marchán, *Mol. Pharmaceutics*, 2013, **10**, 1964; (c) Y. Jin, J. A. Cowan, *J. Am. Chem. Soc*., 2005, **127**, 8408; (d) R. K. Gupta, R. Pandey, G. Sharma, R. Prasad, B. Koch, S. Srikrishna, P. Z. Li, Q. Xu, D. S. Pandey, *Inorg. Chem*., 2013, **52**, 3687.

4 (a) D, Palanimuthu, S. V. Shinde, K. Somasundaram, A. G. Samuelson, *J. Med. Chem*., 2013, **56**, 722; (b) V. Rajendiran, R. Karthik, M. Palaniandavar, H. Stoeckli-Evans, V. S. Periasamy, M. A. Akbarsha, B. S. Srinag, H. Krishnamurthy, *Inorg. Chem*., 2007, **46**, 8208; (c) S. Ramakrishnan, D. Shakthipriya, E. Suresh, V. S. Periasamy, M. A. Akbarsha, M. Palaniandavar, *Inorg. Chem*., 2011, **50**, 6458; (d) A. Barve, A. Kumbhar, M. Bhat, B. Joshi, R. Butcher, U. Sonawane, R. Joshi, *Inorg. Chem*., 2009, **48**, 9120; (e) M. Ganeshpandian, R. Loganathan, S. Ramakrishnan, A. Riyasdeen, M. A. Akbarsha, M. Palaniandavar, *Polyhedron*, 2013, **52**, 924.

5 (a) S. Ramakrishnan, V. Rajendiran, M. Palaniandavar, V. S. Periasamy, B. S. Srinag, H. Krishnamurthy, M. A. Akbarsha, *Inorg. Chem*., 2009, **48**, 1309; (b) B. Maity, M. Roy, S. Saha, A. R. Chakravarty, *Organometallics*, 2009, **28**, 1495; (c) B. Maity, M. Roy, B. Banik, R. Majumdar, R. R. Dighe, A. R. Chakravarty, *Organometallics*, 2010, **29**, 3632; (d) B. Selvakumar, V. Rajendiran, P. U. Maheswari, H. Stoeckli-Evans, M. Palaniandavar, *J. Inorg. Biochem*., 2006, **100**, 316; (e) V. Gandin, M. Porchia, F. Tisato, A. Zanella, E. Severin, A. Dolmella, C. Marzano, *J. Am. Chem. Soc*., 2013, **56**, 7416.

6 (a) P. Smoleński, S. W. Jaros, C. Pettinari, G. Lupidi, L. Quassinti, M. Bramucci, L. A. Vitali, D. Petrelli, A. Kochela, A. M. Kirillovd, *Dalton Trans*., 2013, **42**, 6572; (b) R. Loganathan, S. Ramakrishnan, E. Suresh, M. Palaniandavar, A. Riyasdeen, M. A. Akbarshae, *Dalton Trans*., 2014, **43**, 6177; (c) M. González-Álvarez, A. Pascual-Álvarez, L. C. Agudo, A. Castiñeiras, M. Liu-González, J. Borrása, G. Alzuet-Piña, *Dalton Trans*., 2013, **42**, 10244.

7 (a) P. Jaividhya, R. Dhivya, M. A. Akbarsha, M. Palaniandavar, *J. Inorg. Biochem*., 2012, **114**, 94; (b) J. Hernández-Gil, S. Ferrer, A. Castiñeiras, M. Liu-González, F. Lloret, Á. Ribes, L. Coga, A. Bernecker, J. C. Mareque-Rivas, *Inorg. Chem*., 2014, **53**, 578; (c) Y. An, M. L. Tong, L. N. Ji, Z. W. Mao, *Dalton Trans*., 2006, 2066; (d) N. Raman, R. Mahalakshmi, *Inorg. Chem. Commun*., 2014, **40**, 157; (e) S. Tabassum, M. Zaki, M. Afzal, F. Arjmand, *Eur. J. Med. Chem*., 2014, **74**, 509; (f) H. S. Lee, P. G. Schultz, *J. Am. Chem. Soc*., 2008, **130**, 13194; (g) T. K. Goswami, B. V. Chakravarthi, M. Roy, A. A. Karande, A. R. Chakravarty, *Inorg. Chem*., 2011, **50**, 8452; (h) S. Dhar, M. Nethaji, A. R. Chakravarty, *Inorg. Chem*., 2005, **44**, 8876; (i)A. Prisecaru, V. McKee, O. Howe, G. Rochford, M. McCann, J. Colleran, M. Pour, N. Barron, N. Gathergood, A. Kellett, *J. Med. Chem*., 2013, **56**, 8599.

8 M. Chen, M.-Z. Chen, C.-Q. Zhou, W.-E. Lin, J.-X. Chen, W.-H. Chen, Z.-H. Jiang, *Inorg. Chim. Acta*, 2013, **405**, 461.

9 M. E. Reichmann, S. A. Rice, C. A. Thomas, P. J. Doty, *J. Am. Chem. Soc*., 1954, **76**, 3047.

10 J.-X. Chen, H.-Q. Zhao, H.-H. Li, S. L. Huang, N. N. Ding, W.-H Chen, D. J. Young, W. H. Zhang, T. S. Andy Hor, *CrystEngComm*., 2014, **16**, 7722.

11 G. M. Sheldrick, SADABS. Program for empirical absorption correction of area detector data, University of Göttingen, Germany. 1996.

12. G. M. Sheldrick, SHELXS-97 and SHELXL-97. Programs for crystal structure solution and refinement. University of Göttingen, Germany. 1997.

13. L. J. Farrugia, J. Appl Crystallogr 1999, **32**, 837.

14 (a) C.-Q. Zhou, Y.-L. Lin, J.-X. Chen, L.-S. Wang, N.-N. Yang, W. Zeng, W.-H. Chen, *Bioorg. Med. Chem. Lett*., 2012, **22**, 5853; (b) C.-Q. Zhou, Y.-L. Lin, J.-X. Chen, W.-H. Chen, *Chem. Biodiv*., 2012, **9**, 1125; (c) M. S. Deshpande, A. A. Kumbhar, A. S. Kumbhar, M. Kumbhakar, H. Pal, U. B. Sonawane, R. R. Joshi, *Bioconjugate Chem*., 2009, **20**, 447; (d) W. Zhou, X. Y. Wang, M. Hu, Z. J. Guo, *J. Inorg. Biochem*., 2013, **121**, 114; (e) Y. M. Wang, C. Q. Zhou, J. X. Chen, Y. L. Lin, W. Zeng, B. C. Kuang, W. L. Fu, W. H. Chen, *Med. Chem. Commun*. 2013, **4**, 1400.

15 J.-Y. Pang, Y. Qin, W.-H. Chen, G.-A. Luo, Z.-H. Jiang, *Bioorg. Med. Chem*., 2005, **13**, 5835.

16 (a) L. Xu, N. J. Zhong, Y. Y. Xie, H. L. Huang, G. B. Jiang, Y. J. Liu, *PLoS One*, 2014, **9**, e96082; (b) G. Sathyaraj, M. Kiruthika, T. Weyhermüller, B. U. Nair, *Dalton Trans*., 2012, **41**, 8460; (c) P. Smoleński, S. W. Jaros, C. Pettinari, G. Lupidi, L. Quassinti, M. Bramucci, L. A. Vitali, D. Petrelli, A. Kochela, A. M. Kirillovd, *Dalton Trans*., 2013, **42**, 6572.

17. J. X. Chen, X. Y. Tang, Y. Chen, W. H. Zhang, L. L. Li, R. X. Yuan, Y. Zhang, J. P. Lang, *Cryst. Growth Des.*, 2009, **9**, 1461.

18. J.-X. Chen, M. Chen, N.-N. Ding, W.-H. Chen, W.-H. Zhang, T. S. Andy Hor, D. J. Young, *Inorg. Chem*., 2014, **53**, 7446.
19 (a) J. Kleinberg, *Inorg. Syn*., New York, McGraw-Hill, 1963. (b) E. Gianasi, M. Wasil, E. G. Evagorou, A. Keddle, G. Wilson, R. Duncan, *Eur. J. Cancer*, 1999, **35**, 1002.
20. L. M. Wan, H. X. Li, W. Zhao, H. Y. Ding, Y. Y. Fang, P. H. Ni, J. P. Lang, *J. Polym. Sci., Part A: Polym. Chem*., 2012, **50**, 4864.
21. F. L. Hu, W. Wu, P. Liang, Y. Q. Gu, L. G. Zhu, H. Wei, J. P. Lang, *Cryst. Growth Des*., 2013, **13**, 5050.
22 (a) P. A. N. Reddy, B. K. Santra, M. Nethaji, A. R. Chakravarty, *J. Inorg. Biochem*., 2004, **98**, 377; (b) L. Tjioe, T. Joshi, J. Brugger, B. Graham, L. Spiccia, *Inorg. Chem*., 2011, **50**, 621; (c) S. Rajalakshmi, T. Weyhermüller, A. J. Freddy, H. R. Vasanthi, B. U. Nair, *Eur. J. Med. Chem*., 2011, **46**, 608; (d) S. S. Bhat, A. A. Kumbhar, H. Heptullah, A. A. Khan, V. V. Gobre, S. P. Gejji, V. G. Puranik, *Inorg. Chem*., 2011, **50**, 545; (e) T. K. Goswami, B. V. S. K. Chakravarthi, M. Roy, A. A. Karande, A. R. Chakravarty, *Inorg. Chem*., 2011, **50**, 8542.
23 (a) V. Rajendiran, R. Karthik, M. Palaniandavar, H. Stoeckli-Evans, V. S. Periasamy, M. A. Akbarsha, B. S. Srinag, H. Krishnamurthy, *Inorg. Chem*., 2007, **46**, 8208; (b) A. Barve, A. Kumbhar, M. Bhat, B. Joshi, R. Butcher, U. Sonawane, R. Joshi, *Inorg. Chem*., 2009, **48**, 9120; (c) P. Jaividhya, R. Dhivya, M. A. Akbarsha, M. Palaniandavar, *J. Inorg. Biochem*., 2012, **114**, 94; (d) B. Selvakumar, V. Rajendiran, P. U. Maheswari, H. Stoeckli-Evans, M. Palaniandavar, *J. Inorg. Biochem*., 2006, **100**, 316; (e) P. Krishnamoorthy, P. Sathyadevi, A. H. Cowley, R. R. Butorac, N. Dharmaraj, *Eur. J. Med. Chem*., 2011, **46**, 3376.
24 (a) G. K. Schroeder, C. Lad, P. Wyman, N. H. Williams, R. Wolfenden, *Proc. Natl. Acad. Sci*. USA, 2006, **103**, 4052; (b) W. Xu, J. A. Craft, P. R. Fontenot, M. Barens, K. D. Knierima, J. H. Albering, F. A. Mautner, S. S. Massoud, *Inorg. Chim. Acta*, 2011, **373**, 159.
25. J.-X. Chen, W.-E. Lin, M.-Z. Chen, C.-Q. Zhou, Y.-L. Lin, Z.-H. Jiang, W.-H. Chen, *Bioorg. Med. Chem. Lett*. **2012**, *22*, 7056.
26 (a) M. Roy, R. Santhanagopal, A. R. Chakravaty, *J. Chem. Soc., Dalton Trans*., 2009, **32**, 1024; (b) L. J. K. Boerner, J. M. Zaleski, *Curr. Opin. Chem. Bio*., 2005, **9**, 135.
27 (a) S. Megha, A. A. Deshpande, A. S. Kumbhar, *Inorg.Chem*., 2007, **46**, 5450; (b) D. S. Sigman, A. Mazumder, D. M. Perrin, *Chem. Rev*., 1993, **93**, 2295.
28 (a) M. González-Álvarez, A. Pascual-Álvarez, L. C. Agudo, A. Castiñeiras, M. Liu-González, J. Borrása, G. Alzuet-Piña, *Dalton Trans*., 2013, **42**, 10244; (b) G. J. Chen, Z. G. Wang, X. Qiao, J. Y. Xu, J. L. Tian, S. P. Yan, *J. Inorg. Biochem*., 2013, **127**, 39; (c) C. Icsel, V. T. Yilmaz, A. Golcu, E. Ulukaya, O. Buyukgungor, *Bioorg. Med. Chem. Lett*., 2013, **23**, 2117; (d) J Zhao, S. H. Gou, F. Liu, Y. Y. Sun, C. Z. Gao, *Inorg. Chem*., 2013, **53**, 8163; (e) F. Hackenberg, H. Müller-Bunz, R. Smith, W. Streciwilk, X. M. Zhu, M. Tacke, *Organometallics*, 2013, **32**, 5551; (f) H. Goitia, Y. Nieto, M. D. Villacampa, C. Kasper, A. Laguna, M. C. Gimeno, *Organometallics*, 2013, **32**, 6069; (g) D. Palanimuthu, S. V. Shinde, K. Somasundaram, A. G. Samuelson, *J. Med. Chem*., 2013, **56**, 722; (h) B. Cvek, V. Milacic, J. Taraba, Q. P. Dou, *J. Med. Chem*., 2008, **51**, 6256; (i) L. K. Filak, D. S. Kalinowski, T. J. Bauer, D. R. Richardson, V. B. Arion, *Inorg. Chem*., 2014, **53**, 6934; (j) D. Mavrynsky, J. Rahkila, D. Bandarra, S. Martins, M. Meireles, M. J. Calhorda, I. J. Kovács, I. Zupkó, M. M. Hänninen, R. Leino, *Organometallics*, 2013, **32**, 3012.
29. V. Gandin, M. Porchia, F. Tisato, A. Zanella, E. Severin, A. Dolmella, C. Marzano, *J. Med. Chem*., 2013, **56**, 7416.